International Journal of Recent Advances in Multidisciplinary Topics
Volume 2, Issue 9, September 2021
https://www.ijramt.com | ISSN (Online): 2582-7839

Algorithm for Computation of Troposphere Delay for Navigation and RADAR Stations

Akhilesh Kumar*
Space Navigation Group, U. R. Rao Satellite Centre, ISRO, India

***Abstract*: Troposphere delay is one of the crucial factors of the atmospheric delays of the signal. The troposphere delay directly affects the line-of-sight error of the pseudo range measurements. A generalized model has been used to compute troposphere delay at a specific epoch. This model contains hydrostatic and non-hydrostatic components along with its gradient. The standard Saastamoinen model of troposphere delay can be derived from this generalized model. An algorithm is developed to compute the troposphere delay along with met sensor data using the generalized model. The met sensor data are obtained using three approaches. The first approach is the empirical model, the second approach is grid-based and the last one is real data. Results were obtained with a generalized troposphere model using all three approaches of met sensor data for the IGS (International GNSS Service) ground station. Results compared with the precise troposphere delay and found to be in good agreement. The accuracy is found to be within 28 cm. It can be concluded that the generalized troposphere is reliable and can be used for the correction in the line-of-sight error of the pseudo range measurement. A sensitivity analysis has been performed for troposphere delay to find the sensitive parameters. It has been found that the water vapor decrease factor is the most sensitive parameter among met sensor parameters (i.e., pressure, temperature, water vapor pressure), mean temperature and water vapor decrease factor. The water vapor pressure is the most sensitive among the met sensor parameters. The temperature is the least sensitive among all considered parameters. Also, the present algorithm is used to compute the troposphere delay for NavIC (Navigation with Indian Constellation) system and RADAR (Radio Detection And Ranging) angle measurements. Finally, Troposphere delay is computed for real met sensor data (i.e., Approach 3) and compared with the results of the other two approaches. It has been found that due to uncertainty in the met sensor data, differences vary up to meter level.**

***Keywords*: Met Sensor Data, NavIC, Sensitivity Analysis, Troposphere Delay.**

1. Introduction

Several layers of the atmosphere exist. The troposphere is one of the layers in the atmosphere. The electromagnetic signal transmits from the satellite and is received by the receiver. The travel time of the signal multiplied by the velocity of light gives the pseudo range [1]. However, the received signal is delayed by clocks, ephemeris and atmosphere propagation delay (i.e., Ionosphere and Troposphere). When the signal passes through the troposphere. The signal refracts from its original path in the troposphere layer. This refraction is due to the variations in the temperature, pressure, and water vapor pressure in the Troposphere. As a result, refraction causes a delay in the signal while reaching its destination i.e., user/stations and known as troposphere delay. This delay has prominent effects on satellite transmission signals. This delay is one of the important parameters for pseudo range measurement. The troposphere is not a dispersive medium up to the frequency of 15GHz [23]. Commonly the frequency of the transmit signal in the navigation systems is less than 15GHz. So, tropospheric delay error is independent of the frequency of the signal. The delay caused by Troposphere is eliminated using troposphere delay models.

Several models such as Saastamoinen, Hopfield, Marini Murray, etc. are available to describe the troposphere delay [2],[3]. The troposphere consists of dry and wet constituents that affect the propagation delay of radio frequency signals. So, the available models describe the dry/hydrostatic and wet/non-hydrostatic parts along with the mapping function. The dry portion consists of empirical constants and pressure, latitude, the altitude at the location of the receiver. The wet component consists of temperature and water vapor pressure at the receiver's location along with empirical constants. Several mapping functions like the inverse of sine/cosine of zenith angle, a combination of sine and tangent of zenith angle, continued fraction with the several coefficients are available [2],[3]. The coefficients are empirically determined constants or functions of variables such as latitude, height, surface temperature, pressure, and day of the year [10].

The present work has been divided into five sections. Section 2 describes the theory of the generalized troposphere model. Section 3 describes the algorithm steps to compute the troposphere delay using a generalized model and three different approaches to obtain the met sensor data. Section 4 describes the results obtained using the algorithm of troposphere delay for IGS, NavIC and RADAR stations. Results of troposphere delay compared with existing results of precise troposphere delay of IGS. Section 5 concludes with the major findings.

2. Theory

The Troposphere delay computation algorithm provides the delay caused when the signal from a satellite to the user/Radar (2-way or 1-way) travels through the troposphere. Troposphere delay is one of the parameters of Pseudorange measurement. The troposphere delay algorithm computes the troposphere

*Corresponding author: akhileshisac@gmail.com

delay at an epoch using the general troposphere delay model. The computed troposphere delay can be used for the data processing algorithm, orbit determination, and navigation solution.

The troposphere delay can be computed using mathematical models such as the Saastamoinen model [3],[5] with NEILL mapping function, which will be applied for RADAR/ground measurements. Mathematically, the troposphere delay from the space object (SO) to the RADAR/user/ground station (Rx) can be expressed as [11]

$$T_{Rx}^{SO}\left(t_{Rx},elv_{Rx}^{SO},Az_{Rx}^{SO}\right) = m_h\left(elv_{Rx}^{SO}\right)ZHD_{t_{Rx}} + m_w\left(elv_{Rx}^{SO}\right)ZWD_{t_{Rx}} + mGh\left(elv_{Rx}^{SO}\right)\begin{pmatrix} Gh_{ns_{t_{Rx}}}\cos\left(Az_{Rx}^{SO}\right) \\ +Gh_{ew_{t_{Rx}}}\sin\left(Az_{Rx}^{SO}\right)\end{pmatrix} + mGnh\left(elv_{Rx}^{SO}\right)\begin{pmatrix} Gnh_{ns_{t_{Rx}}}\cos\left(Az_{Rx}^{SO}\right) \\ +Gnh_{ew_{t_{Rx}}}\sin\left(Az_{Rx}^{SO}\right)\end{pmatrix}, \quad (1)$$

where, $T_{Rx}^{SO}\left(t_{Rx},elv_{Rx}^{SO},Az_{Rx}^{SO}\right)$ is the total troposphere delay (m) at each line of sight from the space objects to RADAR/user/ground station with time t_{Rx}, elevation elv_{Rx}^{SO}, and azimuth Az_{Rx}^{SO} angles,

$m_h\left(elv_{Rx}^{SO}\right)$ is the hydrostatic mapping function (-) with elv_{Rx}^{SO}

$m_w\left(elv_{Rx}^{SO}\right)$ is the non-hydrostatic (wet) mapping function (-) at elevation angle elv_{Rx}^{SO},

$ZHD_{t_{Rx}}$ is the hydrostatic delay component (m) at elevation angle elv_{Rx}^{SO},

$ZWD_{t_{Rx}}$ is the wet (non-hydrostatic) component (m) at elevation angle elv_{Rx}^{SO},

$mGh\left(elv_{Rx}^{SO}\right)$ is the hydrostatic gradient mapping function (-) at elevation angle elv_{Rx}^{SO},

$Gh_{ns_{t_{Rx}}}$ is the north-south hydrostatic gradient (m) at time t_{Rx},

$Gh_{ew_{t_{Rx}}}$ is the east-west hydrostatic gradient (m) at time t_{Rx},

$mGnh\left(elv_{Rx}^{SO}\right)$ is the non-hydrostatic gradient mapping function (-) at elevation angle elv_{Rx}^{SO},

$Gnh_{ns_{t_{Rx}}}$ is the north-south non-hydrostatic gradient (m) at time t_{Rx},

$Gnh_{ew_{t_{Rx}}}$ is the east-west non-hydrostatic gradient (m) at time t_{Rx}.

The first two terms of the governing Eq. (1) are dry/hydrostatic and wet/non-hydrostatic components of the troposphere delay and the next two terms are due to hydrostatic gradient components and the last two terms are due to non-hydrostatic gradient components. Here, the modeling approach developed by Saastamoinen (as described in [3]) is followed for the hydrostatic delay component and can be expressed as:

$$ZHD_{t_{RX}} = 0.0022768 \times P\left(1 + 0.00266 \times \cos(2\varphi) + 0.28 \times 10^{-6} h_{ell}\right), \quad (1)$$

Where P is the pressure (mbar),

φ is the geodetic latitude (degree), and

h_{ell} is the geodetic height of the Radar (m).

The Zenith wet/non-hydrostatic delay ($ZWD_{t_{Rx}}$) can be written as [4]:

$$ZWD_{t_{RX}} = 10^{-6} \times \left(k_2^{'} + \frac{k_3}{T_m}\right) \times \frac{R_d e}{g_m(\lambda+1)}, \quad (2)$$

Where e is the water vapor pressure (mbar),

T_m is the mean temperature (Kelvin) weighted with water vapor pressure and λ is the water vapor decrease factor,

$k_2^{'} = k_2 - mk_1$,

$k_1 = 77.60, k_2 = 64.8, k_3 = 3.776 \times 10^5$, ([9]) are the empirically determined refractivity constants $\left[KhPa^{-1}\right]$,

m is the ratio of the molar mass of water vapor and dry air,

R_d is the specific gas constant for dry constituents which equals 287.0464 $JK^{-1}kg^{-1}$, and

g_m is the mean gravity which equals 9.80665 ms^{-2}.

The hydrostatic mapping function ($m_h\left(elv_{Rx}^{SO}\right)$) can be written as [7], [8], and [10]

$$m_h\left(elv_{Rx}^{SO}\right) = \frac{1 + \dfrac{a_h}{1 + \dfrac{b_h}{1 + c_h}}}{\sin\left(elv_{Rx}^{SO}\right) + \dfrac{a_h}{\sin\left(elv_{Rx}^{SO}\right) + \dfrac{b_h}{\sin\left(elv_{Rx}^{SO}\right) + c_h}}}, \quad (3)$$

where $a_h, b_h\left(=0.0029\right)$ and c_h are the coefficients of the hydrostatic mapping function. The a_h Coefficient is determined using the procedure given in the flow chart. The c_h coefficient is determined using the following formulation

$$c_h = c_{0h} + \left(\left(\cos\left(2\pi DOY/365.25 + p_{hh}\right) + 1\right)c_{11h}/2.0 + c_{10h}\right)\left(1 - \cos\varphi\right), \quad (4)$$

Where $c_{0h}\left(=0.062\right)$ is the coefficient. P_{hh}, c_{10h}, c_{11h} coefficients values defined based on the southern and northern hemisphere. If the latitude of the ground station is less than zero then the southern hemisphere and $P_{hh} = \pi, c_{10h} = 0.007, c_{11h} = 0.002.$ Otherwise, northern hemisphere and $P_{hh}=0, c_{10h}=0.005, c_{11h}=0.001$. Finally, the value of c_h can be determined using Eq. (5)

Similarly, the wet (non-hydrostatic) mapping function can be written as given in Eq. (4)

$$m_w\left(elv_{Rx}^{SO}\right)=\frac{1+\frac{a_w}{1+\frac{b_w}{1+c_w}}}{sin\left(elv_{Rx}^{SO}\right)+\frac{a_w}{sin\left(elv_{Rx}^{SO}\right)+\frac{b_w}{sin\left(elv_{Rx}^{SO}\right)+c_w}}}, \quad (5)$$

Where $a_w, b_w\left(=0.00146\right)$ and $c_w\left(=0.04391\right)$ are the coefficients of the wet mapping function. The a_w Coefficient is determined using the procedure given in the flow chart.

Also, the Earth's atmosphere is spatially inhomogeneous having a higher refractive index than free space. So, the transmit signal propagating through this medium will have a decrease in velocity contaminating the measurements. The gradient mapping function for hydrostatic and non-hydrostatic components are as follows [11]

$$mGh\left(elv_{Rx}^{SO}\right)=m_h\left(elv_{Rx}^{SO}\right)\cot\left(elv_{Rx}^{SO}\right)\left(1-10^{-6}N\cos ec^2\left(elv_{Rx}^{SO}\right)\right), \quad (6)$$

$$mGnh\left(elv_{Rx}^{SO}\right)=m_w\left(elv_{Rx}^{SO}\right)\cot\left(elv_{Rx}^{SO}\right)\left(1-10^{-6}N\cos ec^2\left(elv_{Rx}^{SO}\right)\right), \quad (7)$$

Where, N is the total refractivity ([9]) and is expressed as

$$N=k_1\frac{p_d}{T}Z_d^{-1}+k_2\frac{p_{wv}}{T}Z_{wv}^{-1}+k_3\frac{p_{wv}}{T^2}Z_{wv}^{-1}, \quad (8)$$

$$Z_d^{-1}=1+p_d\left[57.9\times10^{-8}\left(1+\frac{0.52}{T}\right)-9.4611\times10^{-4}\frac{t}{T^2}\right], \quad (9)$$

$$Z_{wv}^{-1}=1+1650\left(\frac{p_{wv}}{T^3}\right)\left[1-0.01317\times t+1.757\times10^{-4}t^2+1.44\times10^{-6}t^3\right], \quad (10)$$

Where p_d is the partial pressure of dry air (mbar),

p_{wv} is the partial water vapor pressure (mbar),

Z_d is the compressibility factor of dry air (-),

Z_{wv} is the compressibility factor of water vapor (-),

t is the temperature in degree Celsius $\left(0^0+273.15=273.15\,\text{Kelvins}\right)$,

T is temperature (Kelvins).

Eq. (1) computes the troposphere delay if all the parameters/variables are known as described in Eqns. (2) – (10). The standard grid values contain five coefficients such as mean values $\left(A_0\right)$, as well as sine and cosine amplitudes for the annual $\left(A_1 \text{ and } B_1\right)$, and semi-annual variation $\left(A_2 \text{ and } B_2\right)$. These are the list of parameters available at a grid point with five coefficients at a step size of 1^0 grid: Pressure (Pascal), temperature (Kelvin), specific humidity (kg/10^3 kg), temperature lapse rate (Kelvin/km), geoid undulation (m), orthometric grid height (m), hydrostatic mapping function coefficient (-), wet mapping function coefficient (-), water vapor decrease factor (-), mean temperature (Kelvin), hydrostatic and wet north gradients (m), hydrostatic and wet east gradients (m).

To deduce any parameters $\left(Y\right)$ at any specific grid points the following empirical formula is used as described by [10]:

$$\begin{aligned}Y&=A_0+A_1\cos\left(\frac{2\pi\,DOY}{365.25}\right)+B_1\sin\left(\frac{2\pi\,DOY}{365.25}\right)\\&+A_2\cos\left(\frac{4\pi\,DOY}{365.25}\right)+B_2\sin\left(\frac{4\pi\,DOY}{365.25}\right),\end{aligned} \quad (11)$$

in which A_0 represents the mean value,

A_1 and B_1 the annual amplitudes,

A_2 and B_2 the semi-annual amplitudes,

DOY is the Day Of Year.

The pressure (*P*), temperature (*T*), and partial vapor pressure (*e*) are not directly determined from the grid values, it uses some standard formulas [4] and derives the values $\left(T_G^{'}, P_G^{'}, e_G^{'}\right)$ at the grid point:

$$\begin{aligned}T_G^{'}&=T_G-\frac{\alpha}{1000}\left(h^{'}-h_G\right),\\P_G^{'}&=P_G e^{-\left(\frac{g_m m_a}{R_e T_V}\left(h^{'}-h_G\right)\right)},\\e_G^{'}&=e_G\left(\frac{P}{P_G}\right)^{(\lambda+1)},\end{aligned} \quad (12)$$

where, α is the temperature lapse rate (Kelvin/km),

$h^{'}\left(=h_{ell}-u_G\right)$ is the orthometric height (m),

u_G is the geoid undulation at the grid point (m),

h_G is the height at the grid point (m),

$m_a\left(=0.02897\,kg/mol\right)$ is the molar mass of the air,

$R_g\left(=8.3413\,JK^{-1}mol^{-1}\right)$ is the universal gas constant,

$T_V\left\{=T_G\left(1+0.61q_G\right)\right\}$ is the virtual temperature (Kelvins),

q_G is the specific humidity (kg/10^3kg),

$e_G=q_G\,P_G/\left(0.622+0.328q_G\right)/100$, is the partial vapor pressure at grid points (mbar),

P_G, T_G, e_G are the pressure, temperature, water vapor pressure at the grid points.

The final values of the parameters pressure (P), temperature (*T*), and water vapor pressure (e), are determined using Eq. (12) and Eq. (13) followed by Bilinear interpolation [17]. Other parameters mean temperature (T_m), water vapor decrease factor (λ), hydrostatic coefficient a_h, wet coefficient a_w, hydrostatic and non-hydrostatic east-west $\left(Gh_{ew_{tRx}}, Gnh_{ew_{tRx}}\right)$, and north-south components $\left(Gh_{ns_{tRx}}, Gnh_{ns_{tRx}}\right)$ are determined using Eq. (12) followed by Bilinear interpolation [17].

Further, the hydrostatic (m_h) and wet (m_w) mapping functions are determined using a_h, a_w from Eqs. (4) and (6) respectively. Then mGh and $mGnh$ are determined from Eq. (7) and (8) respectively. The $ZHD_{t_{RX}}$ and $ZWD_{t_{RX}}$ components are determined using Eq. (2) and (3) respectively. Finally, the troposphere delay can be computed using Eq. (1).

It is easy to see that the general troposphere model presented in Eq. (1) reduces to the standard Saastamoinen model if the gradient component is zero (i.e., $mGh=0$ and $mGnh=0$) and also dry and wet mapping functions are equal to the inverse of cosine of zenith angle. It has also been found that Eq. (3) is equivalent to the wet part of the Saastamoinen model [3]. Hence, the standard Saastamoinen troposphere model can be obtained from the generalized troposphere model given by Eq. (1).

3. Algorithm

An algorithm has been developed to compute the troposphere delay using the generalized troposphere model and also shown in the flow chart (i.e., Fig. 1). The following steps are followed to compute the troposphere delay:

1. In the first step, the following inputs are required to compute the troposphere delay:
    a) Station coordinates are in the ECEF (Earth Centred Earth Fixed) frame of reference,
    b) The positions of the satellite/space object are in the ECEF frame of reference,
    c) Time at which troposphere delay has to be computed
2. The geodetic coordinates i.e., (latitude, longitude, and altitude) are calculated from ground station coordinates i.e., (x, y, z) ([3], [13]) using the following mathematical formulas:

Table 1
Bounds for different tropospheric parameters

S.No.		Minimum	Maximum
1.	Azimuth Angle (deg)	0^0	360^0
2.	Elevation Angle (deg)	7^0	90^0
3.	Latitude (deg)	-90^0	90^0
4.	Longitude (deg)	0^0	360^0
5.	Altitude (km)	-3.5	6.2
6.	Pressure (mbar)	460	1509
7.	Temperature (^{0}C)	-20.3	42.75
8.	Troposphere delay (m)	2	27

a) Compute Latitude of ground station/RADAR:

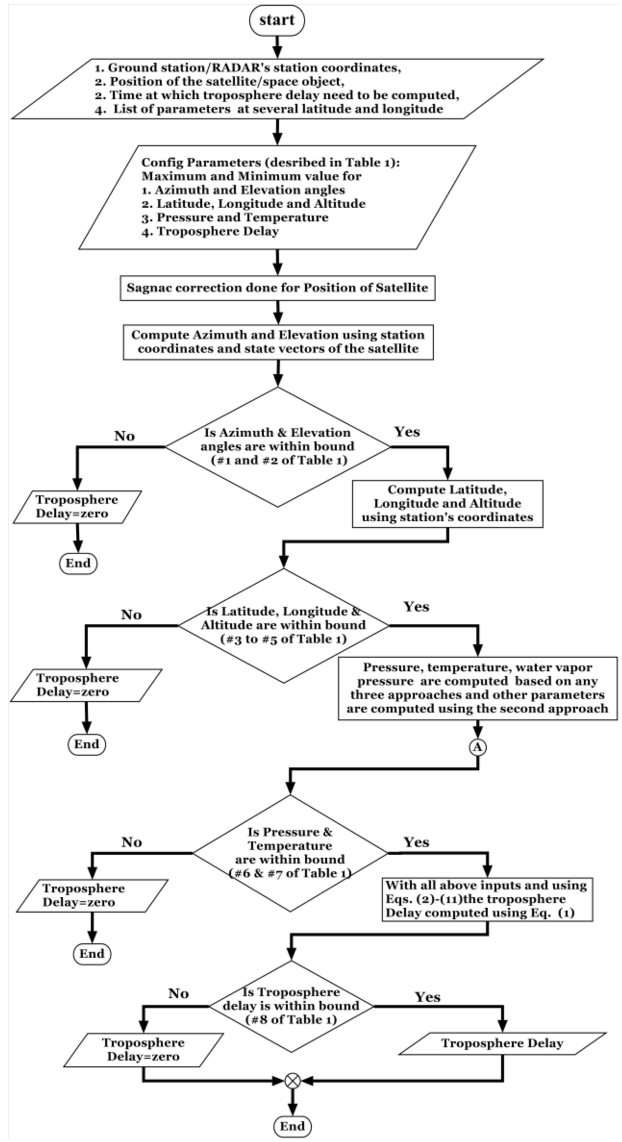

Fig. 1. Flow Diagram to compute the troposphere delay using generalized troposphere model Eq. (1)

$$
\begin{aligned}
&Latitude0 = \tan^{-1}\left(z \big/ \sqrt{x^2+y^2} \big/ \left(1-2f+f^2\right)\right),\\
&where,\ f = \text{Earth Flattering Constant},\\
&while\left(\left|Latitude - Latitude0\right| < 10^{-10}\right)\\
&\qquad Latitude0 = Latitude\\
&\qquad N = R_{\oplus} \big/ \sqrt{\left(1-\left(2f-f^2\right)\sin^2\left(Latitude\right)\right)}\\
&\qquad Latitude = \tan^{-1}\left(\left(z+\left(2f-f^2\right)N\sin\left(Latitude\right)\right) \big/ \sqrt{x^2+y^2}\right)\\
&end
\end{aligned}
\tag{14}
$$

Where, N is the curvature, $R_{\oplus}\left(=6378.137\,km\right)$ is the Earth's radius, $f\left(=1/298.257222101\right)$ is Earth's flattering constant.

b) Compute longitude of ground station/RADAR:

$$\begin{aligned}&Longitude = tan^{-1}\left(y/x\right),\\&if\ Longitude < 0\ then\ Longitude = Longitude + 2\pi.\end{aligned} \quad (15)$$

c) Compute altitude of the ground station/RADAR:

$$\begin{aligned}&if\ Latitude <= (160\pi/360)\\&\quad Altitude = \sqrt{x^2+y^2}\Big/\cos(Latitude) - N\\&else\\&\quad Altitude = z\Big/\sin\left(Latitude\right) + N\left(2f - f^2 - 1\right)\\&end\end{aligned} \quad (16)$$

3. The Sagnac correction is applied to the position of GPS satellites [12].
4. The azimuth and elevation angles are computed using station coordinates i.e., (x, y, z) and position of the satellite coordinates i.e., (x_S, y_S, z_S) [13] using the following mathematical formula:

$$Elevation = \frac{\pi}{2} - \cos^{-1}\left(\frac{(\vec{r}_s - \vec{r})\cdot\vec{r}}{|\vec{r}_s - \vec{r}||\vec{r}|}\right) \quad (17)$$

$$Azimuth = atan2\begin{pmatrix}(\vec{r}_S - \vec{r})\bullet\\(\sin(Longitude),\cos(Longitude),0),\\(\vec{r}_S - \vec{r})\end{pmatrix}, \quad (18)$$

$$if\ Azimuth < 0,\ Azimuth = Azimuth + 2\pi$$

5. Met data (pressure, temperature, and water vapor pressure) at geodetic coordinates can be obtained using the following three approaches.

Approach 1: The 1st approach follows the standard empirical atmospheric model [14] and the expressions are as follows:

$$\begin{aligned}&if\ \left(Altitude > -10000m\ \&\ Altitude < 10000m\right)\\&\quad P = P_{Reference}\left(1 - 0.0000226\,Altitude\right)^{5.225},\\&\quad T = T_{Reference} - 0.0065Altitude,\\&\quad RH = RH_{Reference}e^{-0.0006396\,Altitude}.\\&else\\&\quad P = P_{Reference},\\&\quad T = T_{Reference},\\&\quad RH = RH_{Reference},\\&end\\&if\ RH > 100,\ RH = 100.\end{aligned} \quad (19)$$

Where (P, T, RH) is the pressure, temperature, and relative humidity, $(P, T, RH)_{Reference}$ is the reference pressure, temperature and, relative humidity with its values $P_{Reference}$ =1013.25mbar, $T_{Reference} = 20^0C$, and $RH_{Reference} = 50\%$. The temperature from ^0C is converted into ^0K using $T = 273.15 + T$. The water vapor pressure is computed as:

$$e = \left(Altitude/100\right)\exp\begin{bmatrix}-37.2465\\+0.213266T\\-0.000256908T^2\end{bmatrix} \quad (20)$$

To compute the troposphere delay using a generalized model, all other parameters are obtained from the 2nd approach.

Approach 2: In the 2nd approach, met parameters along with other parameters are obtained at geodetic coordinates from standard grid values. These are the list of parameters available at a grid point with a step size of 1^0: Pressure (Pascal), temperature (Kelvin), specific humidity (kg/10^3kg), temperature lapse rate (Kelvin/m), geoid undulation (m), orthometric grid height (m), hydrostatic mapping function coefficient (-), wet mapping function coefficient (-), water vapor decrease factor (-), mean temperature (Kelvin), hydrostatic and wet north gradients (m), hydrostatic and wet east gradients (m)[10]. The standard grid values at latitude [-89.5^0,89.5^0] and longitude [0.5^0,359.5^0] with the 1^0x1^0grid have been used. The standard grid values contain five coefficients. The one coefficient represents the mean values of the coefficient. The two more coefficients denote the annual amplitude of the coefficients. The last two coefficients stand for the semi-annual amplitude of the coefficients. Using these coefficients, the met parameters are obtained as mentioned in the flowchart (i.e., Fig. 2).

Approach 3: In the 3rd approach, real data of pressure, temperature, and relative humidity [22] are used. The water vapor pressure is computed using Eq. (20). All other parameters are obtained from the 2nd approach (Fig. 2) to compute the troposphere delay using a generalized model.

With all the above steps and using Eqs. (2)-(11), the troposphere delay is computed using the generalized Eq. (1).

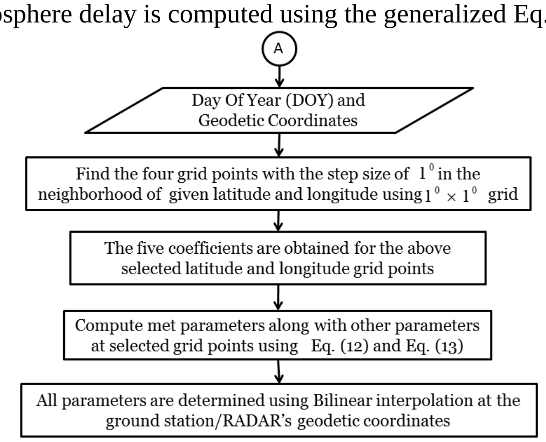

Fig. 2. Flow Diagram to compute the met parameters along with other parameters at the geodetic coordinates using grid-based values

4. Results and Analysis

The developed algorithm in this study is used to compute the troposphere delay of the IGS, NavIC and RADAR stations. Results obtained for troposphere delay are compared with the precise troposphere delay. A sensitivity analysis is performed for various tropospheric parameters. Further, the tropospheric delay has also been computed with the real meteorological sensor data and compared with the results of IGS.

1) *Troposphere Delay for IGS Ground Stations*

To evaluate the troposphere delay, precise products of troposphere delay and the position of the satellites are used in this study. The precise troposphere delay for various IGS stations is collected from CDDIS for a specific Day Of Year (DOY)) [18]. Also, the precise orbit of the satellites is obtained from the CDDIS for a specific week number and time of week [18]. In this article, the two data sets are used i.e., precise troposphere delay and precise orbit are obtained for DOY 101 to DOY 105, 2021 for more than 400 IGS stations. The precise orbit is available in SP3 file format and precise troposphere delay is available in SINEX format. The details of formats for both data sets are available in [19].

The troposphere delay is computed for all the IGS stations using the generalized troposphere model. To compare the computed troposphere delay with the precise one the following steps have been followed:

1. The precise troposphere delay is available at the interval of 5 minutes and the precise orbits are available at the interval of 15 minutes. To compute the troposphere delay using a generalized troposphere model the position of GPS satellites is required at the interval of 5 minutes. So, Lagrange's interpolation [16] has been used to compute at the interval of 5 minutes.
2. The Sagnac correction is applied to the position of GPS satellites.
3. The geodetic coordinates (latitude, longitude, and altitude), elevation, and azimuth angles are computed as described in the algorithm using the station position provided in the SINEX file of the troposphere.
    1. The met sensor data are obtained using three approaches as mentioned in the algorithm.
    2. The troposphere delay is computed using Eq. (1) with all the above inputs and using Eqs. (2) -(11).
    3. Finally, the computed troposphere delay is converted into zenith troposphere delay and compared with the precise total zenith troposphere delay.

Table 2
Results of different statistical metrics for troposphere delay for few IGS stations

IGS station name	**Mean of difference (m)**	**Std of difference (m)**	**Mean % of dry**	**Mean % of wet**	**Std of gradient (m)**	**Std of % gradient**
Abmf	-0.0487	0.0436	91.3954	8.6046	0.0017	0.0134
Abpo	-0.0314	0.0295	93.2286	6.7714	0.0005	0.0048
Acrg	0.0339	0.0281	87.8336	12.1664	0.0006	0.0049
Aggo	0.0200	0.0492	93.5693	6.4307	0.0024	0.0201
Aira	-0.0270	0.0607	94.4962	5.5038	0.0042	0.0367
Ajac	-0.0063	0.0331	94.9738	5.0262	0.0013	0.0107
Albh	0.0179	0.0211	95.4645	4.5355	0.0015	0.0132
Algo	-0.0215	0.0198	95.9500	4.0500	0.0013	0.0149
Alic	-0.0122	0.0381	94.3251	5.6749	0.0022	0.0194
Amc4	-0.0117	0.0189	96.2257	3.7743	0.0012	0.0136
Ankr	-0.0101	0.0151	90.8036	9.1964	0.0013	0.0115
Anmg	-0.0127	0.0192	87.6440	12.3560	0.0012	0.0090
Antc	0.0037	0.0197	96.6195	3.3805	0.0026	0.0259
Areg	-0.0131	0.0322	95.3463	4.6537	0.0062	0.0683
Areq	-0.0146	0.0318	95.3458	4.6542	0.0062	0.0683
Arht	-0.0047	0.0118	99.5622	0.4378	0.0008	0.0068

As real met data is not available for all IGS stations. So, the troposphere delay is computed using Eq. (1) with Approaches 1 and 2. Now, results are presented only for the second approach in Table 2. Later, in subsection 4.5., for few IGS stations real met sensor data is obtained from [22] and discussed. The mean, standard deviation (std), maximum (max) and minimum (min) are used as a statistical metric to characterize the results. The mean and standard deviation (std) are calculated for the compared results (i.e., the difference of computed and precise troposphere delay) for DOY 101 to DOY 105, 2021. Also, the percentage of dry, wet, and gradient components are computed for various IGS stations. Also, mean and std are computed for dry, wet and gradient components. It has been found that the mean is sufficient to describe the percentage (i.e., %) of dry and wet components across all IGS stations. Also, it has been noticed that the mean of the gradient components and their % are negligible. So, only the std of gradient components are presented in Table 2. Results are computed for all available precise troposphere IGS stations. But results are presented in Table 2 for few IGS ground stations. The mean and std show good agreement between computed and precise troposphere delays.

The max and min values are found for all components of troposphere delay (shown in Table 2) across all IGS stations. Results are presented in Table 3. This table depicts that the max difference is 0.23 m and the min difference is -0.28 m across all IGS stations. The max of dry component is 99.7451 % and the min of dry component is 86.1357%. The max of wet component is 13.8643% and the min of wet component is 0.2549%. The max and min value of gradient component is 15mm and 0.4mm respectively among all IGS stations. The max of gradient component is approximately 0.1% and the min of gradient component is 0.0029%. Results can be obtained for multiple GPS satellites and various IGS stations simultaneously.

Table 3
Maximum and Minimum of all components presented in Table 1 across all IGS stations

Max of the difference (m)	**Min of the difference (m)**	**Max of gradient (m)**	**Min of gradient (m)**	**Max of dry component (%)**
0.2334	-0.2802	0.0155	0.0004	99.7451
Min of dry component (%)	Max of wet component (%)	Min of wet component (%)	Max of gradient (m)	Min % of gradient (m)
86.1357	13.8643	0.2549	0.0992	0.0029

2) Sensitivity Analysis

A sensitivity analysis is performed to identify the critical parameters for the troposphere delay. Sensitivity is the partial derivative of the troposphere delay with respect to a change in the value of a parameter [15].

$$s_{ij} = \frac{\partial T_{Rx_i}^{SO}}{\partial p_j} \quad (21)$$

Where s_{ij} is the sensitivity of troposphere delay $T_{Rx_i}^{SO}$ to the parameter p_j. Sensitivities of pressure (P,mbar), temperature (T, kelvin), water vapor pressure (e,mbar), mean temperature (T_m, Kelvin), and water vapor decrease factor (λ, -) are calculated for various IGS stations from DOY 101 to 105, 2021. Results are presented in Table 4. From the results, it is clear that maximum change in the troposphere delay is due to the parameter λ and minimum change in the troposphere delay due to the parameter T. So, λ is most sensitive and T is the least sensitive parameters among all these parameters. Table 4 also depicts that change in troposphere delay is maximum for water vapor pressure among the met sensor parameters (i.e., P, T and e). So, water vapor pressure (i.e., e) is the most sensitive parameter.

3) Troposphere Delay for NavIC ground station

NavIC stands for Navigation with Indian Constellations. NavIC consists of eight operational satellites. These satellites are equipped with OCXO/Rubidium atomic clocks. NavIC also consists of 17 ground stations. These stations are equipped with hydrogen maser/cesium/rubidium atomic clocks [21]. In this article, troposphere delay computed only for those satellites driven by rubidium atomic frequency standards and the stations equipped with hydrogen maser/cesium atomic clocks. So, troposphere delay was computed for nine NavIC ground stations using the algorithm of generalized troposphere delay from Doy 101 to Doy 105, 2021. Results are presented in Table 5. This table shows the maximum and minimum elevation angles and corresponding troposphere delay. Table 5 shows the minimum elevation angle is 9.93^0 and the maximum elevation angle is 88.34^0. The corresponding value of troposphere delay is 12.43m and 2.2m respectively.

Table 4

Maximum $\left(dT_{Rx_{max}}^{SO}\right)$ and Minimum $\left(dT_{Rx_{min}}^{SO}\right)$ values of Sensitivity of Troposphere delay to the parameters p_j

p_j	$dT_{Rx_{min}}^{SO}$ (m)	$dT_{Rx_{max}}^{SO}$ (m)	$dT_{Rx_{max}}^{SO} - dT_{Rx_{min}}^{SO}$
P	0.0023	0.0174	0.0151
T	-0.00009195	0.00008868	0.00018062
e	0.0087	0.1449	0.1362
T_m	0.0001	0.0357	0.0355
λ	-0.7237	-0.0044	0.7193

Time vs elevation angle and Time vs troposphere delay has been shown for Bangalore station for Doy 101 and Doy 102, 2021. From the figure and Table, it is clear that when the elevation angle is minimum then the troposphere delay is maximum and vice versa.

Table 5

Results for NavIC ground stations from Doy 101 to 105, 2021

NavIC Stations	Min Elevation (Degree)	Troposphere delay (m)	Max Elevation (Degree)	Troposphere delay (m)
Bangalore	28.2177	4.5813	75.7120	2.2331
Bhopal	19.5101	6.7529	75.6934	2.2332
Hassan	27.2106	4.6268	74.7871	2.2410
Port Blair	20.6844	6.8211	74.3360	2.2651
Mahendragiri	32.1099	4.5477	80.2592	2.2106
Shillong	16.3667	7.3489	72.7767	2.5477
Jodhpur	14.5350	9.3120	74.3315	2.4441
Lucknow	18.1650	7.6661	72.4365	2.2520
Mauritius	9.9253	12.4333	88.3398	2.2032

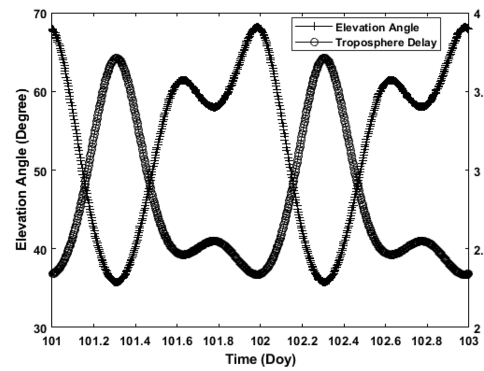

Fig. 3. A typical plot for Time vs troposphere delay and Time vs Elevation angle for Bangalore station for Doy 101 and Doy 102, 2021

4) Troposphere Delay for RADAR ground station

A multi-object tracking radar (MOTR) was established at SDSC SHAR, ISRO. This radar is capable of track multi-space objects and provides range and angular measurements. The angular measurements (i.e., elevation and azimuth angles) are available for a few of the Indian Satellites from 4th September 2021 to 8th September 2021 [20]. In this article, the angular measurements are used to compute the troposphere delay using the algorithm of a generalized model as described in the previous sections. Results are presented in Table 6. This table shows the max and min elevation angles and corresponding troposphere delay. It is clear from the table that the min elevation angle is 19.23^0 and the max elevation angle is 42.05^0. The corresponding delay value is 7.88m and 3.91m respectively. It has also been found that approximately 87.3% for a max of dry component and 12.7% for a max of the wet component. The Max value of the gradient component is 0.06 mm and 0.01%. Results agree well with the results of IGS and NavIC ground stations.

5) Troposphere Delay with real met data

The real met sensor data (i.e., pressure, temperature and humidity) was obtained from [14] for the following IGS ground stations: Abpo, Abmf, Acrg, Aggo, Aira, Ajac, Albh, Algo, Alic and Auck. These datasets are available in the local time and offsets from UTC is also available [22]. So, to use these met data at UTC, offsets are applied. The met data are available with an interval of 30mins. So, the troposphere delay computed using Eq. (1) with all three approaches of met sensor data. It has been observed that the difference in the three approaches of troposphere delay is more than a meter. This is due to the uncertainty of the meteorological parameters. Results are shown in Table 7 for the water vapor pressure because of the most sensitive parameter in the met sensor parameters.

Table 6
Results for tacked space objects by MOTR from 4^{th} September to 8^{th} September, 2021

Date	Name of Space Objects	Min Elevation (Degree)	Tropo delay (m)	Max Elevation (Degree)	Tropo delay (m)
04/09/2021	Cartosat 2e	27.7200	5.6132	38.7200	4.1846
06/09/2021	Cartosat 3	33.8100	4.7000	81.9400	2.6485
06/09/2021	Risat 2b	28.0400	5.5550	86.1800	2.6282
07/09/2021	Risat 2b	25.5700	6.0445	52.4000	3.3076
08/09/2021	Megha-Tropiques	42.0500	3.9097	79.0500	2.6708
08/09/2021	Cartosat 3	19.2300	7.8849	76.7200	2.6942
08/09/2021	Cartosat 2e	33.9900	4.6782	72.8400	2.7441

Results for the water vapor pressure calculated from Eq. (20) for all three approaches are shown in Fig. 4. Although results are computed for all mentioned IGS stations but for clarity, one IGS station Ajac has shown in Fig. 4. It depicts that the water vapor pressure is almost as a constant using Approaches 1 and 2 but not a constant throughout a day for IGS ground station using Approach 3. It is well known that the meteorological data is not a constant for a user/ground station/RADAR location for one day. So, Approach 3 is more accurate compare to Approaches 1 and 2.

Table 7
Results for IGS ground stations from Doy 101 to 105, 2021

IGS stations	Approach 1		Approach 2		Approach 3	
	Min WVP (mbar)	Max WVP (mbar)	Min WVP (mbar)	Max WVP (mbar)	Min WVP (mbar)	Max WVP (mbar)
Abpo	2.2735	2.2735	14.4158	14.7357	15.1271	20.9169
Abmf	12.1682	12.1684	23.9820	24.2334	18.3344	32.3711
Acrg	10.8436	10.8445	28.9127	28.9174	28.5339	34.2748
Aggo	11.3651	11.3653	15.1616	15.6492	10.5517	24.7126
Aira	8.5151	8.5152	10.9571	11.4317	5.6395	21.8070
Ajac	10.6831	10.6832	11.2878	11.6580	6.2705	16.2918
Albh	11.4597	11.4597	7.8529	7.9700	3.7231	9.5167
Algo	9.5966	9.5967	5.2751	5.7352	3.6320	7.4224
Alic	6.2781	6.2781	8.4185	8.6714	5.6866	14.3736
Auck	10.3097	10.3098	13.8660	14.1116	14.1208	23.6942

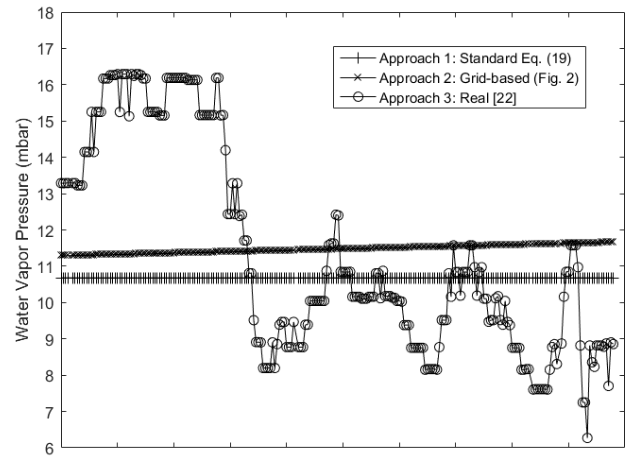

Fig. 4. Water vapor pressure using all three approaches for Ajac IGS ground station from Doy 101-105, 2021

5. Conclusion

A generalized troposphere model is proposed to calculate the troposphere delay using met sensor data. Three different approaches are proposed to get the met sensor data. The results are analyzed for all three methods. The second approach is more realistic when compared to the standard atmospheric model. In the case of Approach 2, the met parameters are defined as trigonometric functions, which are based on the latitude and longitude of the user. However, due to the uncertainty of the meteorological parameters, the third approach is more accurate compared to the two approaches. The proposed model is used for the evaluation of tropospheric delays for different navigation systems such as NavIC and IGS. The delay is also computed for real data of RADAR. Finally, the present troposphere model is performed for few IGS stations with real meteorological data.

The present tropospheric model is verified through the precise measurement of the troposphere delay using IGS products. It achieves good accuracy within 28cm. It has been found that the dry component is varied from 86.14% to 99.75% and the wet component is varied from 0.25% to 13.86%. The gradient component contribution in the troposphere delay is only a few mm. A sensitivity analysis has been performed to find the most and least sensitive parameters for troposphere delay. It has been found that the water vapor decrease factor is the most sensitive parameter and temperature is the least sensitive parameter. It has been found that the minimum elevation angle is approximately 9.93^0 and the maximum elevation angle is 88.34^0 for NavIC ground stations. Results of NavIC and RADAR ground stations agree well with the results of IGS.

Acknowledgement

The authors are highly grateful to Smt. Nirmala S and Smt. Anatta Sonney, of Space Navigation Group, U. R. Rao Satellite Centre, ISRO for their constant support and inspiration throughout this work.

References

[1] A. Leick, "Pseudorange and Carrier Phase Observables," in GPS Satellite Surveying 2nd Edition, Wiley, New York, 1994.

[2] Bradford W Parkinson, James J Spilker, “The Tropospheric effects on GPS” global positioning system: theory and applications, Volume I. Part II : GPS performance and error effects, Washington, DC : American Institute of Aeronautics and Astronautics, January 1, 1996.

[3] Misra, Pratap and Per, Enge, “*GPS Measurements and error sources*,” Global Positioning System: Signals, Measurements, and Performance, Ganga-Jamuna Press, 2012.

[4] Askne J, Nordius H, “Estimation of tropospheric delay for microwaves from surface weather data,” *Radio Science*, vol. 22, no. 3, pp. 379–386, 1987.

[5] Saastamoinen J, “Atmospheric correction for the troposphere and stratosphere in radio ranging of satellites,” *The use of artificial satellites for geodesy*, vol. 15, pp. 247–251, 1972.

[6] Davis JL, Herring TA, Shapiro II, Rogers AEE, Elgered G, “Geodesy by radio interferometry: effects of atmospheric modeling errors on estimates of baseline length,” Radio Science, vol. 20, no. 6, pp. 1593–1607, 1985.

[7] Marini JW, “Correction of satellite tracking data for an arbitrary tropospheric profile,” Radio Science, vol. 7, no. 2, pp. 223–231, 1972.

[8] Niell AE, “Global mapping functions for the atmosphere delay at radio wavelengths,” J Geophysical Research, vol. 101, pp. 3227–3246, 1996.

[9] Thayer, G.D., “An improved equation for the radio refractive index of air,” Radio Science, Vol. 9, No. 10, pp. 803-807, 1974.

[10] Daniel Landskron and Johannes Böhm, “VMF3/GPT3: Refined Discrete and Empirical Troposphere Mapping Functions,” *J Geodesy*, vol. 92, pp. 349-360, 2018.

[11] Reza Ghoddousi-Fard, “Modelling Tropospheric gradients parameters from NWP models: Effects on GPS estimates,” Ph.D. dissertation, Department of Geodesy and Geomatics Engineering, University of New Brunswick, Fredericton, New Brunswick, Canada, 216 pp, 2009.

[12] Z. Hecimovic, Relativistic effects on satellite navigation. Tehnicki Vjesnik, 2013; 20(1): 195-203, 2021

[13] J. Sanz Subirana, J.M. Juan Zornoza and M. Hernández-Pajares, “*B Coordinate Conversions*,” GNSS DATA PROCESSING: Volume I: Fundamentals and Algorithms, ESA Communications, 2013.

[14] Berg H, “Allgemeine Meteorologie,” Dümmler, Bonn, 1948.

[15] Wagner BJ, Harvey JW, “Experimental Design for estimating parameters of rate-limited mass transfer: analysis of stream tracer studies,” Water Resources Research, vol. 33, no. 7, pp. 1731-1741, 1997.

[16] Abramowitz, Milton*;* Stegun, Irene Ann,. "*Chapter 25, eqn 25.2.3*". Handbook of Mathematical Functions with Formulas, Graphs, and Mathematical Tables*.* Washington D.C.; New York, p. 878,1983.

[17] https://en.wikipedia.org/wiki/Bilinear_interpolation.

[18] https://cddis.nasa.gov/archive/gnss/products/.

[19] https://files.igs.org/pub/data/format/

[20] https://en.wikipedia.org/wiki/Indian_Space_Research_Organisation

[21] https://www.isro.gov.in/irnss-programme

[22] https://www.timeanddate.com/weather/

[23] https://gssc.esa.int/navipedia/index.php/Tropospheric_Delay/